Kufa Journal of Engineering
Vol. 16, No. 2, April 2025, P.P. 249 -262
Article history: Received 28 March 2024, last revised 5 October 2024, accepted 6 October 2024

ROBUST SLIDING-MODE-BASED LEARNING FOR MAXIMUM POWER POINT TRACKING PHOTOVOLTAICS SYSTEM

Abdal-Razak Shehab Hadi [1*], Adnan Alamili [2] ,and Ali Abdyasser Kadhum [3]

[1] Electrical Engineering Department, Faculty of Engineering, University of Kufa, Kufa, Iraq. E-mail: abdulrazzaq.aljuburi@uokufa.edu.iq.

[2] Electrical Engineering Department, Faculty of Engineering, University of Kufa, Kufa, Iraq. E-mail:adnan.alaamili@uokufa.edu.iq .

[3] Electric Technical Department, Kufa Technical Institute, Al-Furat Al-Awsat Technical University, Iraq. E-mail: kin.ali1@atu.edu.iq.

https://doi.org/10.30572/2018/KJE/160215

ABSTRACT

Maximum power point tracking (MPPT) is crucial for optimizing the energy extraction from solar modules in photovoltaic (PV) systems. This paper focuses on maximizing the energy extraction from solar panels and explores the important aspects of MPPT technology in PV systems. The sliding mode learning controller (SMLC) created for MPPT provides a new way to deal with environmental factors, including radiation and temperature fluctuations. The study compares the disturbance-insensitive SMLC with linear proportional-integral-derivative (PID) controllers and conventional sliding mode controllers (CSMC). The SMLC enhances the maximum energy extraction by tracking the reference voltage signal using the perturb and observe (P&O) algorithm. Moreover, the controller can adapt to the dynamic changes in PV characteristics thanks to the learning system. The result shows that the proposed SMLC offers significant benefits, especially in challenging operating conditions. It demonstrates superior vibration-free performance, fast response (with a settling time of 24.7 ms), and smooth and precise tracking compared to other controllers.

KEYWORDS

Photovoltaic system, Maximum power point tracking (MPPT), Perturb and observe (P&O) algorithm, PID controller, SMLC.

1. INTRODUCTION

Given the huge impact of greenhouse gas emissions and the increasing cost of traditional fuel, PV systems have shown up as an alternative. As sustainable energy sources, PV systems provide many advantages, including minimal maintenance, no moving parts, low noise, zero fuel costs, and the operation of pollution-free pollution. These attributes make them more advantageous than conventional techniques (Subudhi and Pradhan, 2012; Mao et al., 2020a) .

In developing countries, likewise in rural and small urban communities, small-scale PV systems often meet daily energy consumption needs. Conversely, developed countries are embracing clean energy in regions with high solar radiation (Sawin et al., 2013). The power-voltage curve is vital to represent the performance of PV systems, espitially the maximum power output, defined as the maximum power point (MPP). This curve usually has a single peak, but under partial shade conditions (PSCs), diurnal activity or seasonal changes, it can present multiple nonlinear peaks. This poses challenges for conventional MPPT methods to capture the MPP. A study was conducted to characterize and summarize MPPT innovations for PV systems based on control theories and optimization principles (Mao et al., 2020b).

Given the rapid changes in solar radiation and the resulting impact on performance, extensive research has been conducted on the effectiveness of the traditional P&O algorithm, especially in its response to changes in radiation levels. A P&O algorithm-based MPP tracer was proposed and evaluated (Anon., n.d.). Furthermore, the fuzzy logic (FL) control in conjuction to the P&O algorithm has been investegated. The advantage of P&O-MPPT in this combination used to manage both rapid and gradual variations in solar radiation. FL-MPPT's faster processing time increases its usefulness (Abdel-Salam, El-Mohandes and Goda, 2018; Al-Majidi, Abbod and Al-Raweshidy, 2018). Furthermore, a thorough evaluation of MPPT techniques, which occupies a contemporary taxonomy focusing on comparative methodologies, has been undertaken. The study explores scenarios where solar PV (SPV) systems are coupled with a switching hybrid active filter (SHAF) to mitigate harmonics and harness active energy (Das et al., 2022). Practitioners are helped to make informed decisions during designing solar systems using Global MPPT (GMPPT) techniques for PV systems under PSCs (Belhachat and Larbes, 2018) (Danandeh, 2018).

Moreover, research on multipoint PV modules using MPPT technologies embedded in commercially available MPPT modules has produced a dynamic technology that optimizes PV power generation through continuous monitoring of MPPT (Dhimish, 2019). An optimal duty cycle is generated by optimizing the fuzzy membership functions (MFs) of MPPT using an optimization technique. Conventional P&O and symmetric fuzzy logic controllers (SFLC) have been the most often used techniques to compare the performance of optimized FLC (Farajdadian and Hosseini, 2019). The convergence requirements of the regular PSO method were analyzed functionally, which led to the development of the improved PSO (IPSO) algorithm. Moreover, the voltage-oriented MPPT (VO_MPPT) technique was established by integrating the traditional P&O algorithm with adaptive integral derivative sliding mode (AIDSM)-based external voltage control (Kihal et al., 2019). Researchers investigated and validated the hybrid between adaptive P&O and PSO using an experimental prototype integrated into a PV array simulator. This hybrid uses a search, skip, and judge (SSJ) mechanism, and was tested using four popular MPPT methods: hybrid PSO, diversified additive conduction, modified cuckoo search, and the original version of SSJ (Kermadi et al., 2018). Synthesizing electronic power converter control, focusing on improving tracking accuracy, speed, and reliability, a new method for controlling PVs based on neural networks has been established and proposed (Hu et al., 2019; Issaadi, Issaadi and Khireddine, 2019).

Finally, in this research, a hybrid SMLC approach using SMLC for MPPT has been established to effectively and accurately track MPPT in the presence of unknown and unmodeled perturbations. The proposed controller includes a learning control signal base to assist in adapting the duty cycle supply of the DC-to-DC power switch boost converter. This ensures that the controller quickly reaches the global ideal zone. To verify the effectiveness of this innovative MPPT control technology, extensive simulations of the PV system were performed under different radiation and temperature conditions. Standard control methods, such as PID, conventional SMC, AIDS, and SMLC MPPT, were used for comparison. In addition, a comparative analysis of MPPT systems and PV systems operating throughout the day was presented.

The subsequent sections of this research are organized as follows. Section 2 provides the research methodology, including the mathematical modelling of PV cells, a single-diode equivalent circuit of a PV panel, dynamic modelling of the DC to DC boost converter, CSMC and robust SMLC design for MPPT. Additionally, MPPT controllers and the P&O algorithm are discussed, highlighting the benefits of the suggested strategy. Section 3 presents results, emphasizing the effectiveness of the presented controller in different scenarios, followed by a conclusion section that summarizes the findings and identifies possible avenues for future research.

2. RESEARCH METHOD

Enhancing the performance characterization of PV systems is the main aim of this study, with an emphasis on managing unknown and unmodeled disturbances and optimizing energy production. This aim is pursued throughout many steps. Initially, the PV system was dynamically modelled to establish a basis foundation for subsequent analyses. Next, a DC-to-DC boost converter was modelled, and a specialized SMLC was formulated for MPPT in the PV system. A block diagram of comprehensive research methodology, which outlines the sequential steps, is shown in the upcoming subsection.

2.1. Mathematical Model of PV Cells

The development of efficient solar energy systems depends on accurately predicting PV energy production under different environmental conditions and developing effective control strategies, which are crucial to improving their performance. This objective is achieved by incorporating semiconductor physics, solar irradiation, and internal electrical properties to represent the mathematical modelling of PV cells. These mathematical models are a key aspect in simulating the electrical behaviour according to the PV system's voltage and current characteristic curve. A comprehensive analysis is achieved by examination of the solar panel's physical attributes, visualized as an electrical system with both nonlinear as well as linear elements. The SPV elements are a crucial element that employs the direct conversion of the PV effect into electricity within this analysis. Meanwhile, PV arrays are configured by assembling SPV elements in series and parallel constructions, with a P-N junction in most cells presenting. This study adopts a simplified equivalent PV model, known as the single-diode model (SDM) proposed by (Siddiqui et al., 2013), to portray a representative solar cell, as shown in Fig.1.

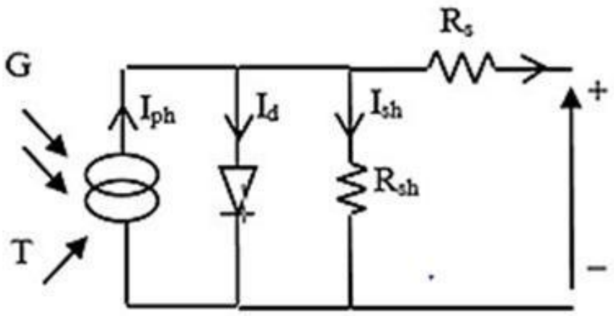

Fig. 1. An equivalent PV electric circuit model.

The I-V characteristic that defines the cell is described by the diode's equivalent circuit shown above as follows:

$$I = I_{ph} - I_0\left[e^{\left(\frac{V+IR_s}{V_t}\right)} - 1\right] - \frac{V+IR_s}{IR_{sh}} \tag{1}$$

where V and I represent the output voltage (V) and output current (A), respectively, of the diode. The I_0 signifies the diode reverse saturation current. And, V_t denotes the thermal voltage, given by V_t = aKT_c/q, where q denotes the electron charge constant, K is the Boltzmann constant, a represents the ideal factor, and T_c denotes the SPV temperature (°C). The serial and parallel resistances denoted by R_s, R_{sh}, respectively are in (Ω). On the other hand, I_{ph} denotes the photocurrent, which is determined by the following formula as a function of the junction temperature and irradiation level (G) (A. Fezzani, 2015):

$$I_{ph} = I_{STC} \frac{G}{G_{STC}} [1 + \alpha(T_C - T_{CSTC})] \qquad (2)$$

where G_{STC} and T_{CSTC} are the irradiance and the temperature of the SPV cell, respectively, at standard test conditions (STC). I_{STC} is the short circuit current at an STC, and α is the current temperature coefficient. The value of the parameter I_0 of the reverse saturation current varies with the cell temperature under STC conditions and can be evaluated as;

$$I_0 = I_{rs} \left(\frac{T_C}{T_{CSTC}}\right)^3 e^{qE_g \frac{\left(\frac{1}{T_C} - \frac{1}{T_{C,STC}}\right)}{Ka}} \qquad (3)$$

where Eg represents the material band-gap energy and I_{rs} is the reverse saturated current at STC. R_s and R_{sh} are determined as in (4) (De Soto, Klein and Beckman, 2006):

$$R_{sh} = R_{sh,STC} \frac{G}{G_{STC}}, R_s = R_{s,STC} \qquad (4)$$

where, at STC conditions, $R_{s,STC}$ and $R_{sh,STC}$ are the serial and shunt resistances, respectively. For a solar cell, Eq.1 remains workable under these conditions. However, the term (V + R_sI) is substituted with ($\frac{V+N_sR_sI}{N_s}$)for a precise application of this equation to the PV module. To determine the five parameters mentioned in Eq.1, involving the representation of I_{ph}, R_s, R_{sh}, I_0, and a, as described by (A. Fezzani, 2015; Fezzani et al., 2016; 2017). To get the necessary voltage for the PV module, Ns cells are usually connected in series. In a series panel, all the cells must have the same current which is the panel current. In this research, the actual shell SPV 1Soltech 1STH-215-P module is used with 47 strings in parallel and 10 modules in series. Table 1 lists the unit's electrical specifications based on the STC model provided by the manufacturer.

Table 1. Data of Array type: 1Soltech 1STH-215-P

No.	Electrical specifications	Value
1	Open circuit voltage (Voc)	36.30 (V)
2	Short-circuit current (Isc)	7.84 (A)
3	Maximal voltage (Vmax)	29.00 (V)
4	Maximal current (Imax)	7.35 (A)
5	Maximal power (Pmax)	213.15 (W)
6	Number of cells (Ns)	36

The module simulated results are presented in Fig.2, and its characteristics are maintained under various levels of temperature and irradiation. The results show the characteristics curves of current-voltage (I-V) and power-voltage (P-V) for various temperatures (i.e., 55ºC, 45ºC, and 25ºC, respectively. These simulation results were implemented within a MATLAB simulation environment.

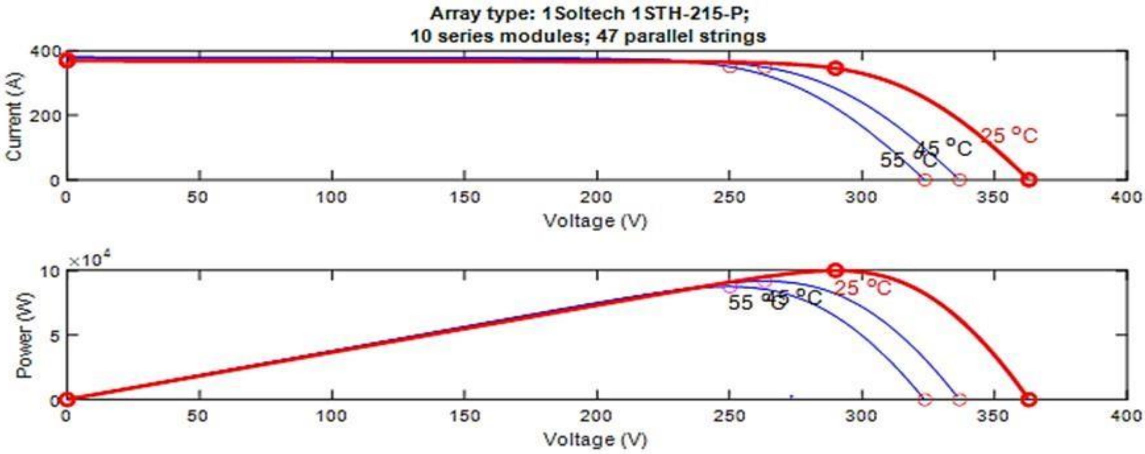

Fig. 2. Simulation results in the test environment (I-V) and (P-V) for (55 45 25) ºC.

2.2. DC-to-DC Boost Converter Dynamic Model

A DC-to-DC boost converter dynamic model is shown for power electronics optimization, and efficient power transmission and control in various applications. Also, a demonstration of the operating mechanism of DC-to-DC boost converters is determined to illustrate their role in driving PV panels to their MPPT. These converters, facilitating energy flow regulation from the PV module to the load, employ a power transistor switch that changes between open and closed states with a fixed-frequency pulse width modulation (PWM) signal. The switch features an adjustable duty cycle (D) within the range of ($0 < D < 1$). The typical DC-to-DC-boost converter is demonstrated in Fig. 3, in which the output/input voltage relation is written as follows:

$$V_o = \frac{1}{1-D} V_{PV} \tag{5}$$

Eq.6 below, defines the model within the state space of the time-invariant nonlinear system.

$$\begin{cases} \dot{X}_1 = \frac{1}{C_1}(I_{PV} - I_L) \\ \dot{X}_2 = \frac{1}{L}(V_{PV} - (1-D)V_o) \\ \dot{X}_3 = \frac{1}{C_2}(-I_o + (1-D)I_L \end{cases} \tag{6}$$

where the states $X_1, X_2, and\, X_3$ indicate the following state system V_{PV}, I_L, and V_o, respectively, C_1 and C_2 function as input and output capacitors. Meanwhile, u will be the control signal which is equivalent to $(1 - D)$, while I_o is the output current, which can be deduced from Ohm's law.

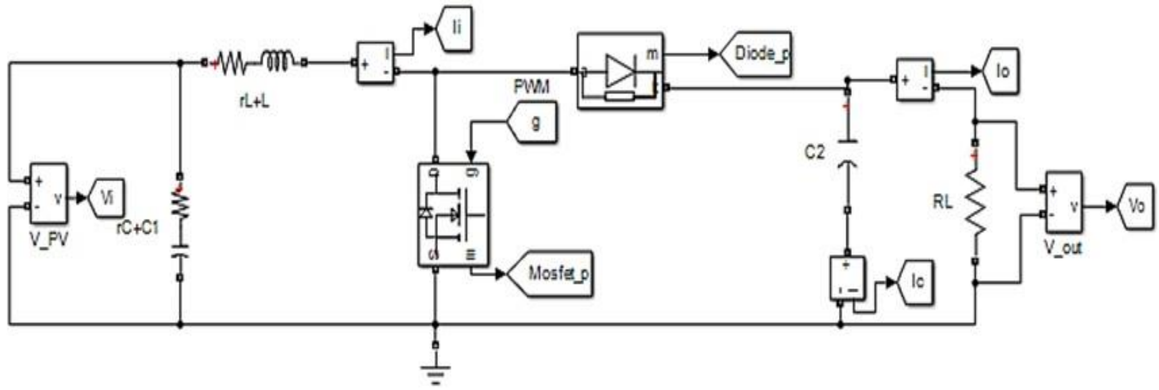

Fig. 3. DC-to-DC boost converter.

2.3. Control Design

In this section, we provide the SMC design for MPPT in PV systems. The robust nature of SMC guarantees stability under disturbance, making it ideal for managing changes in weather patterns. We portray the formulation, slip surface, control regulation, and general control configuration structure for an effective MPPT.

2.3.1. CSMC Design for MPPT

In SMC, states are constrained to be stable in any state space, known as a sliding surface. Thus, when a disturbance happens in the system for any reason, all states are forced to return to the line (S=0) and keep the sliding mode function (S) at zero. While the sliding surface is reached, the controller maintains states near the sliding surface, (S=0) (Utkin, 1978). As a typical feedback control strategy, SMC is broadly used because of exceptional properties permit it to be used in linear and nonlinear systems. This control technology is very suitable for a powerful energy system that functionally varies due to climate differences. The PV system usually depends on weather conditions. Subsequently, embracing these control strategies for a PV system is crucial for accurately monitoring the MPP under varying external conditions. To accomplish this objective, the SMC for the MPPT issue will be figured out. To begin with, the sliding surface is characterized as follows:

$$s(t) = \dot{e}(t) + \lambda e(t) \tag{7}$$

where λ represents a positively valued real constant that governs the incline of the sliding surface, and the tracking error, denoted as $e(t)$, is given as;

$$e(t) = [x_d - x(t)] = V_{ref} - V_{pv} \tag{8}$$

where x_d refers to the desired trajectory generated via the P&O algorithm, V_{ref} denotes the reference voltage, and V_{pv} signifies the output voltage of the PV panel.

Assume that the sliding condition is fulfilled (i.e., s(t) = 0) and solve Eq.7 as a homogeneous linear differential equation. The error tends to approach zero asymptotically for positive values of λ, given the existence of a control law. The Lyapunov functions can be used to get a control law by defining $V(s) = 0.5s^2$ with zero initial conditions, which can deduce the system stability is guaranteed if and only if the adopted controller can guarantee $\dot{V}(t)$ is always decreasing (i.e., < 0). For the nominal condition, this goal would be easy to achieve with a nominal controller which can be inferred by solving $\dot{V}(t) = 0$. However, having a robust controller is crucial for dealing with system uncertainties and external disturbances. Therefore, it is possible to choose the general robust controller rule such as;

$$u(t) = -Ksign(s) \tag{9}$$

in this case, K represents a positively valued real constant with a lower limit determined by the estimated system parameters. The control input, incorporating the sign function, inherently exhibits an intermittent function, resulting in infinite switches along the sliding surface. As a consequence, the path remains consistently constrained to movement along the direction of the sliding surface. There is a significant defect in the SMC called chattering, which occurs with the switching control signal. In our case, we obtain the following expression following the first derivation of the system's output ($\dot{s} = f_1(x, t) + f_2(x, t)u$),

Where ($f_1(x,t) = -\left(\frac{V_{pv}}{LC_2} + \frac{\lambda I_L}{C_2}\right);\ f_2(x,t) = \left(\frac{1}{LC_2} + \frac{\lambda}{R_L C_2}\right) V_o),\ R_L$, is the load resistance.

Assume that the sliding condition is satisfied (i.e., $s(t) = 0$ and $\dot{s}(t) = 0$) and solve Eq.6 as a homogeneous linear differential equation such as;

$$u_{sw}(t) = -(K + \Delta(t))\ sign(s) \tag{10}$$

where $\Delta(t)$, is the uncertainties. The total control signal is defined as, $u = u_{eq.} + u_{sw}$.

2.3.2. Robust SMLC approach for MPPT

The proposed control algorithm is similar to the recursive learning method (Djemaï et al., 2011; Yatimi and Aroudam, 2016), comprising a learning term and a recent control signal. Based on the closed-loop system's most recent stability status, the learning term actively searches for the sliding manifold to optimize stability and convergence. This adjustment capability facilitates the correction of control signals in instances of closed-loop system instability. As a result, the Lyapunov function's gradient value moves from the loop trajectory to achieve and maintain a sliding state. To illustrate, consider the tracking error represented by (8), where V_{ref} denotes the reference voltage, and V_{pv} it signifies the output voltage of the PV panel, and the sliding variable is defined in (7). The time derivative of the sliding variable, s(t) can be expressed as follows:

$$\dot{s}(t) = a(t) + b\,u(t) + \lambda\left(\delta_f(t)\right) \tag{11}$$

Let , then; $a(t) = f_1(x,t), b = f_2(x,t)$

$$f(t) = f_1(x,t) + \lambda\left(\delta_f(t)\right) \tag{12}$$

Where , $\lambda\left(\delta_f(t)\right)$ uncertainty function.

The formula that follows defines the suggested sliding mode learning controller;

$$u(t) = u(t-\tau) - \Delta u(t) \quad (13)$$

Here, the correction term $\Delta u(t)$ in this case is described as;

$$\Delta u(t) = \begin{cases} \frac{1}{bs(t)}\left(\alpha\hat{\dot{V}}(t-\tau) + \beta|\hat{\dot{V}}(t-\tau)|\right) & \text{for } s(t) \neq 0 \\ 0 & \text{for } s(t) = 0 \end{cases} \quad (14)$$

Where τ standing for the time delay, $\hat{\dot{V}}(t-\tau)$ indicates the estimated derivative of the delayed Lyapunov candidate function (i.e., $V(t-\tau) = 0.5\, s(t-\tau)^2$ which is provided as;

$$\hat{\dot{V}}(t-\tau) = \frac{V(t)-V(t-\tau)}{\tau} \quad (15)$$

Meanwhile, α and β are the control parameters to be determined. It should be mentioned that the sample time for actual implementation is assumed to correspond with the minimum value of the time delay τ. If τ is small enough, it makes sense to assume that;

$$sign\left(\hat{\dot{V}}(t-\tau)\right) = sign\left(\dot{V}(t-\tau)\right) \quad (16)$$

$$|\dot{V}(t-\tau) - \hat{\dot{V}}(t-\tau)| < \mu\left|\hat{\dot{V}}(t-\tau)\right| \quad (17)$$

$$For \quad \hat{\dot{V}}(t-\tau) \neq 0, \dot{V}(t-\tau) \neq 0, and\ 0 < \mu \ll 1 \ .$$

Following inequality (17) the difference between the Lyapunov function's gradient and its approximation is minimal since τ is sufficiently small. It appears that (13) and (14) indicate that $u(t)$ is a continuous signal for $s(t) \neq 0$. If $s(t) = 0$, $u(t)$ is continuous at all points. In (14) the suggested SMLC preserves continuity throughout the state space.

2.3.3. The overall control structure.

Fig. 4. shows a schematic representation of the overall control structure, including the electrical circuits of the Shell Solar 1Soltech 1STH-215-P PV module and the PV array module as detailed in Table 1. A DC-to-DC boost converter is configured with an inductance (L) of 1.45 mH, and the capacitances of (C1) and (C2) are 1000μF and 327.7μF, respectively. Additionally, the load resistance (R) is 2Ω and the P&O MPPT algorithm is used. The boost converter switching frequency is adjusted to 25 kHz.

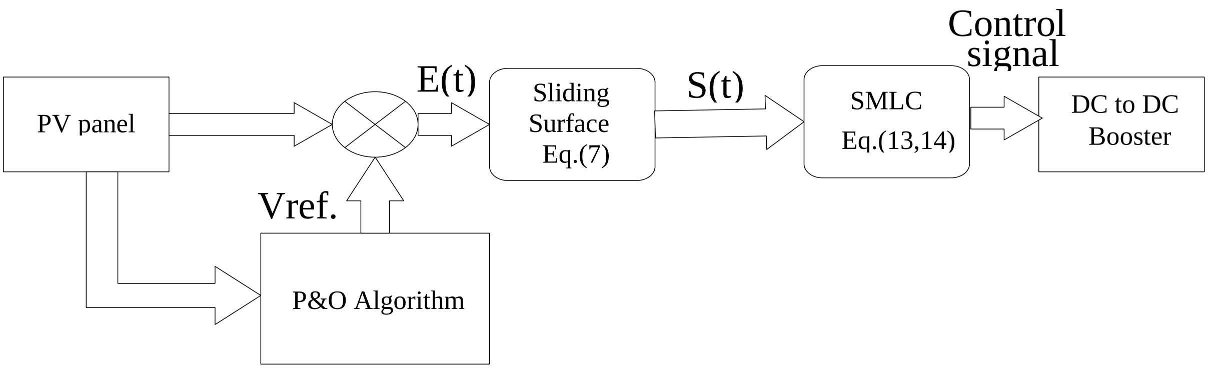

Fig. 4. An illustration of the general control structure.

3. RESULTS AND DISCUSSION

The research includes the design and testing of three different controllers for the PV system, namely a proposed controller, a constrained CSMC, and a linear PID controller. The PID control is expressed in (18) below, where $e(t)$ is the tracking error specified in Eq.7, and Kp, Ki and Kd are the proportional, integral, and derivative gains, respectively.

$$u(t) = Kp\, e(t) + Kd\frac{de(t)}{dt} + Ki\int e(t)dt \quad (18)$$

The auto-tuning feature in the MATLAB simulation environment was utilized to determine the gains of the PI controller in this study (k_p = 0.7, k_i = 10) to minimize steady-state error and enhance system performance. For the conventical sliding mode controller (λ = 1, k =15), and a sliding mode based-learning controller (α = .06, β = .0002). The three controllers were tested under constant irradiation conditions of 1000 W/m2 and temperatures ranging from 25°C to 45°C, reflecting real-world summer day scenarios. Under different temperature conditions and sudden variations, Fig. 5. illustrates the power tracking performance of each controller. CSMC and the proposed controller were tested for their robustness to external disturbances, and both were found to outperform the linear PID controller. The SMLC controller also demonstrates better tracking performance and lessens the chattering effect compared to the other two controllers. The SMLC also eliminates the chattering effect, resulting in smooth tracking performance. However, both CSMC and PID show high ripple for tracking maximum point of power and worse performance.

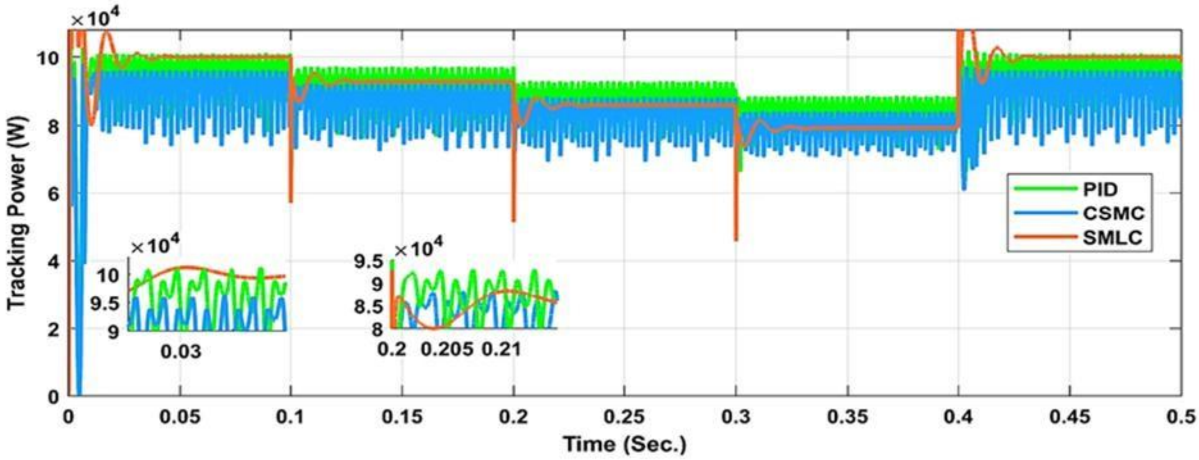

Fig. 5. Simulation results for different types of controllers with constant irradiation (1000 W/m^2) and variable temperatures (25 35 45 25) °C.

Table 2. presents the dynamic response characteristics of the three controllers, including rising time, overshoot, settling time, and steady-state error. The results show that the proposed controller (SMLC) outperforms the other two controllers, with a rising time of 0.00139 sec, overshoot of 1.1%, and settling time of 0.0247 sec. In contrast, both CSMC and PID exhibit a longer settling time and higher overshoot.

Table 2. Dynamic response characteristics of SMLC, CSMC, and linear PID for test 1

Type	Rising time (s)	Overshoot %	Settling time (s)	Steady-state error %
SMLC	0.00139	1.1	0.0247	none
CSMC	0.00139	17.56	infinite	Continue ripple
PID	0.009977	17.56	infinite	Continue ripple

In addition, Fig. 6. shows the simulation results at a constant temperature (25 ℃) with various values of irradiation (i.e., 1000, 750, 500, and 250) W/m2 at a simple time of 0.1 s. This variation can be considered an external disturbance. Interestingly, the results for each control type show a similar trend in terms of the chattering effect and system performance corresponding to the previous results when changing the temperature. The remarkable outcomes observed with the suggested controller can be attributed to the inherent robustness provided by CSMC. The recursive learning techniques are responsible for the continuous tuning of the control signal based on previous control efforts and, as a consequence, system trajectories. Also, the SMLC significantly mitigated the chattering effect compared to the other two controllers (i.e., CSMC, and linear PID). This is due to the sliding variant implicit in the proposed controller design presented in (13). In summary, the proposed SMLC shows excellent performance in handling external disturbances and mitigating the chattering effect. The study's findings suggest that the SMLC hybrid properties could be a significant advantage in the field of power generation control and could be an alternative solution to a typical MPPT system.

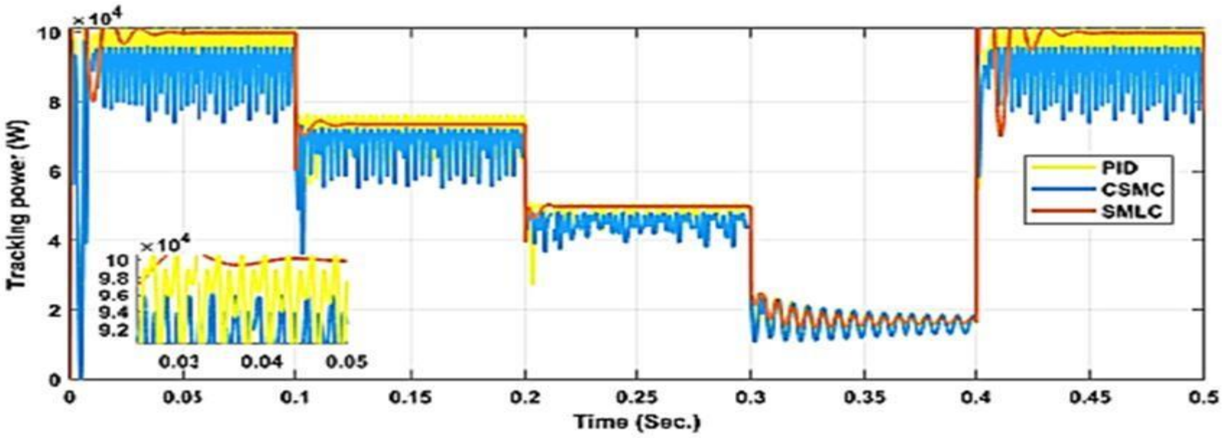

Fig. 6. Simulation results for different types of constant temperature controllers at (25) ºC, and the variable irradiation [1000 750 500 250] W/m^2 in a simple 0.1 s time.

4. CONCLUSIONS

Our paper presents a robust MPPT control approach based on a sliding mode-based learning controller designed for photovoltaic applications, showcasing its efficacy in various operational scenarios. This approach, simulated in MATLAB/Simulink, outperforms traditional PID controllers, ensuring heightened dynamic system performance and efficiency, which is known to be more secure in nonlinear systems. The proposed method exhibits increased robustness against changes in irradiation within variable environments, encompassing variations in both irradiation and temperature. Moreover, the proposed algorithm (SMLC), addresses and mitigates the chattering phenomenon inherent in CSMC due to the switching frequency in sliding mode. Also, CSMC and SMLC treat perturbations as uncertainty or unmodeled rather than the case with the dominant PID controller (PI in this study). It is clear from the result that all types of controllers contribute to an unsteady response when the irradiation is (250 W/m2) due to the principle of the boost converter. This approach is the basis for monitoring the practical implementation of this research work. Furthermore, when implementing the P&O algorithm, it is crucial to consider the P&O step change (P-V curve) for PSC. This ensures that the algorithm calculates from the global maximum point rather than the local maximum issues. In conclusion, the suggested SMLC performs admirably at managing outside disturbances and reducing the chattering effect, quickness of response (settling time (24.7 msec.)) and smooth, precise tracking. The results of the study indicate that the SMLC hybrid features may offer several benefits for controlling power generation and might be used as a substitute for traditional MPPT systems.

ACKNOWLEDGEMENTS

The authors express their gratitude to the University of Kufa, Faculty of Engineering for providing technical assistance, which greatly contributed to the successful completion of this research.

CONFLICT OF INTEREST

The authors have no conflict of relevant interest to this article.

5. REFERENCES

A. Fezzani, I.H.-M.S.D. and L.C.-A., 2015. Modeling and analysis of the photovoltaic array faults. *3rd International Conference on Control, Engineering & Information Technology (CEIT)*, pp.1–9.

Abdel-Salam, M., El-Mohandes, M.-T. and Goda, M., 2018. An improved perturb-and-observe-based MPPT method for PV systems under varying irradiation levels. *Solar Energy*, 171, pp.547–561.

Al-Majidi, S.D., Abbod, M.F. and Al-Raweshidy, H.S., 2018. A novel maximum power point tracking technique based on fuzzy logic for photovoltaic systems. *International Journal of Hydrogen Energy*, 43(31), pp.14158–14171.

Anon. n.d. the effectiveness of the traditional perturbation and observation (P&O) method.

Belhachat, F. and Larbes, C., 2018. A review of global maximum power point tracking techniques of photovoltaic system under partial shading conditions. *Renewable and Sustainable Energy Reviews*, 92, pp.513–553.

Danandeh, M.A., 2018. A comparative and comprehensive review of maximum power point tracking methods for PV cells. *Renewable and Sustainable Energy Reviews*, 82, pp.2743–2767.

Das, S.R., Hota, A.P., Pandey, H.M. and Sahoo, B.M., 2022. Industrial power quality enhancement using fuzzy logic-based photovoltaic integrated with a phase shunt hybrid active filter and adaptive controller. *Applied Soft Computing*, 121, p.108762.

De Soto, W., Klein, S.A. and Beckman, W.A., 2006. Improvement and validation of a model for photovoltaic array performance. *Solar energy*, 80(1), pp.78–88.

Dhimish, M., 2019. Assessing MPPT techniques on hot-spotted and partially shaded photovoltaic modules: Comprehensive review based on experimental data. *IEEE Transactions on Electron Devices*, 66(3), pp.1132–1144.

Djemaï, M., Busawon, K., Benmansour, K. and Marouf, A., 2011. High-order sliding mode control of a DC motor drive via a switched-controlled multi-cellular converter. *International Journal of Systems Science*, 42(11), pp.1869–1882.

Farajdadian, S. and Hosseini, S.M.H., 2019. Optimization of fuzzy-based MPPT controller via metaheuristic techniques for stand-alone PV systems. *International journal of hydrogen energy*, 44(47), pp.25457–25472.

Fezzani, A., Hadj, M.I., Said, D., Zaghba, L., Bouchakour, A., Benbitour, M. and Hamid, O.S., 2017. Degradation and performance evaluation of PV module in desert climate conditions with estimate uncertainty in measuring. *Serbian Journal of Electrical Engineering*, 14(2), pp.277–299.

Fezzani, A., Mahammed, I.H., Drid, S., Bouchakour, A., Zaghba, L., Benbitour, M. and Oudjana, S.H., 2016. Degradation Evaluation of PV Module Using Solmetric PVA-600 Analyzer. In: *4th International Seminar on New and Renewable Energy, Ghardaia, Algeria*. pp.24–25.

Hu, K., Cao, S., Li, W. and Zhu, F., 2019. An improved particle swarm optimization algorithm is suitable for photovoltaic power tracking under partial shading conditions. *IEEE Access*, 7, pp.143217– 143232.

Issaadi, S., Issaadi, W. and Khireddine, A., 2019. New intelligent control strategy by robust neural network algorithm for real-time detection of an optimized maximum power tracking control in photovoltaic systems. *Energy*, 187, p.115881.

Kermadi, M., Salam, Z., Ahmed, J. and Berkouk, E.M., 2018. An effective hybrid maximum power point tracker of photovoltaic arrays for complex partial shading conditions. *IEEE Transactions on Industrial Electronics*, 66(9), pp.6990–7000.

Kihal, A., Krim, F., Laib, A., Talbi, B. and Afghoul, H., 2019. An improved MPPT scheme employing adaptive integral derivative sliding mode control for photovoltaic systems under fast irradiation changes. *ISA transactions*, 87, pp.297–306.

Mao, M., Cui, L., Zhang, Q., Guo, K., Zhou, L. and Huang, H., 2020a. Classification and summarization of solar photovoltaic MPPT techniques: A review based on traditional and intelligent control strategies. *Energy Reports*, 6, pp.1312–1327.

Mao, M., Cui, L., Zhang, Q., Guo, K., Zhou, L. and Huang, H., 2020b. Classification and summarization of solar photovoltaic MPPT techniques: A review based on traditional and intelligent control strategies. *Energy Reports*, 6, pp.1312–1327.

Sawin, J.L., Martinot, E., Barnes, D., McCrone, A., Roussell, J., Sims, R., Sonntag-O'Brien, V., Adib, R., Skeen, J. and Musolino, E., 2013. renewables 2011-Global status report.

Siddiqui, M.U., Arif, A.F.M., Bilton, A.M., Dubowsky, S. and Elshafei, M., 2013. An improved electric circuit model for photovoltaic modules based on sensitivity analysis. *Solar Energy*, 90, pp.29–42.

Subudhi, B. and Pradhan, R., 2012. A comparative study on maximum power point tracking techniques for photovoltaic power systems. *IEEE Transactions on Sustainable Energy*, 4(1), pp.89–98.

Utkin, V.I., 1978. Sliding modes and their applications in variable structure systems. *Mir, Moscow*.

Yatimi, H. and Aroudam, E., 2016. Assessment and control of a photovoltaic energy storage system based on the robust sliding mode MPPT controller. *Solar Energy*, 139, pp.557–568.